Phys. Lett. B 848 (2024) 138340

Contents lists available at ScienceDirect

Physics Letters B

journal homepage: www.elsevier.com/locate/physletb

Letter

A multi-shell extension of the interacting boson model

Feng Pan [a,b,*], Yu Zhang [a], Lianrong Dai [c], Jerry P. Draayer [b], David Kekejian [d]

[a] Department of Physics, Liaoning Normal University, Dalian 116029, China
[b] Department of Physics and Astronomy, Louisiana State University, Baton Rouge, LA 70803-4001, USA
[c] Department of Physics, School of Science, Huzhou University, Huzhou, Zhejiang 313000, China
[d] Department of Physics and Astronomy, University of North Carolina, Chapel Hill, NC 27599, USA

ARTICLE INFO

Editor: B. Balantekin

Keywords:
One-particle-one-hole excitations
Configuration mixing
Extension of the interacting boson model

ABSTRACT

A multi-shell extension of the simplest formulation of the interacting boson model that appends parity-conserving ($2\hbar\omega$) energy excitations to the non-extended theory is proffered. From a physical perspective this extension links the system's low-lying configurations to higher-lying multiple one-particle-one-hole (1p-1h) excitation modes that are in part tethered to the system's isoscalar giant monopole and quadrupole resonances. An application of the theory to low-lying energy levels and known B(E0) and B(E2) values of ^{152}Sm shows that the results obtained with the extension are better than those without the extension.

1. Introduction

It should be clear that in addition to early collective model results [1], the interacting boson model (IBM) [2–4] has enjoyed considerable success in reproducing the low-lying spectra and related features of medium to heavy mass nuclei. The basic assumption that underpins the IBM is that the primary modes of an even-even nucleus can be well represented in terms of a 'boson-based' nuclear economy wherein each boson is considered to be a pair of valence particles or holes. The main advantage of this proxy scheme is that all of the complications associated with managing the requirements of the Pauli-Exclusion Principle that are part-and-parcel of a 'fermion-based' nuclear economy is sidestepped by replacing the latter with a simpler surrogate 'boson-based' nuclear economy. The primary physical feature that underpins this picture is the dominance of pairing correlations in nuclei that is everywhere apparent in low-lying nuclear configurations. Not surprisingly, over time a number of enhancements for cross-shell excitations from below a valence shell have been added to the earliest and simplest versions of the IBM [5–8], in which only multiple two-particle (2p) and two-hole (2h) excitations with 2p and 2h pairs being approximated as s- or d-bosons are considered in elucidating positive parity intruder states and shape coexistence phenomena for nuclei near to a closed-shell [8,9].

The purpose of this paper is to systematically extend the simplest IBM picture by algebraically appending another type of configuration mixing with multiple ($2\hbar\omega$) energy excitations to its valence shell configuration. Similar to multiple 2p-2h excitations from below a valence shell being considered in [5–8], particle-hole excitations with a hole in a given shell and a particle in the upper next nearest shell being approximated as a boson are introduced. The motivation behind this follows from successes realized within the framework of a fermion-based nuclear economy that builds upon the seminal work of J. P. (Phil) Elliott [10], who advanced what is now known as the Elliott SU(3) Model. The fact that SU(3) plays a key role in this model should not come as a surprise because SU(3) is the symmetry group of the 3-dimensional harmonic oscillator (3D-HO); which means that the basis states for any single-shell of the 3D-HO can be decomposed into a direct sum of irreducible representations (irreps) of SU(3), each of which is labeled by (λ, μ). As Elliott - along with others - subsequently showed, an SU(3) irrep can be directly connected to the (β_s, γ_s) shape defining Bohr variables [11] of the Geometrical Collective Model (GCM) [12–14]. Further, within about a decade of Elliott's pioneering work, an extension of the Elliott SU(3) Model that adds ($2\hbar\omega$) oscillator excitations to the theory led to the development of what is now known as the Symplectic Sp(3, **R**) Shell Model [15–19]. From a physical perspective the latter extended Elliott's SU(3) Model, which is a compact group with finite-dimensional irreps, into the non-compact Sp(3, **R**) group structure that has infinite-dimensional irreps, which is essential to gaining a faithful representation of rotational features in nuclei existing in abundance across the Chart of the Nuclides. The ultimate goal of this paper is to establish a complementary algebraic framework to that of the Sp(3, **R**) model building forward from the simplest IBM theory. Since the U(6) symmetry, which

* Corresponding author at: Department of Physics, Liaoning Normal University, Dalian 116029, China.
E-mail addresses: daipan@dlut.edu.cn (F. Pan), draayer@lsu.edu (J.P. Draayer), kekejian@unc.edu (D. Kekejian).

https://doi.org/10.1016/j.physletb.2023.138340
Received 9 October 2023; Received in revised form 15 November 2023; Accepted 15 November 2023
Available online 20 November 2023

serves to define the top-most IBM symmetry structure, includes an embedded SU(3) symmetry limit, it seems that while this may seem to be an ambitious goal, it should be realizable. In what follows we explore how this can be accomplished short of letting the theory push us in the direction of a more complex multiple-mode configurational spatial geometry. Going beyond this would be tantamount to reproducing efforts that have gone into creating the Symmetry Adapted No-Core Shell Model (SA-NCSM) [20–23], which is a fully microscopic fermion-based shell-model theory, but one with rather limited reach due to some untenable complexities that one encounters when attempting to use it for nuclei beyond the *fp*-shell.

2. Theoretical framework

As a first step in this direction, in this paper only s and d bosons are considered. To establish a working notation for achieving a fully boson-base economy that includes the $2\hbar\omega$ excitations, let $s_n^\dagger(s_n)$ and $d_n^\dagger(d_n)$ be the n-th boson creation (annihilation) operators, which are approximated from coupling a particle in the $2n$-th oscillator shell and a hole in the $2(n-1)$-th oscillator shell for $n \geq 1$, and for $n = 0$ the original IBM boson creation (annihilation) operators in the valence shell are recovered; namely, $s_0 = s$ and $d_0 = d$, respectively. It should be noted that to create such 1p-1h pairs is only possible when there are sufficient particles in the $2(n-1)$-th oscillator shell. It follows from this that the Hamiltonian of an extended consistent-Q (CQ) formalism of the IBM that includes these types of $2\hbar\omega$ excitations can be written as

$$\hat{H} = \sum_{n=0}^{P} \left(\varepsilon_{s\,n}\, \hat{N}_{s\,n} + \varepsilon_{d\,n}\, \hat{N}_{d\,n} \right) - \gamma\, \hat{Q} \cdot \hat{Q}, \tag{1}$$

where n labels the $2n$-th oscillator shell with $n = 0$ reserved for the valence shell of the even-even nucleus under consideration, and $\varepsilon_{s\,n}$ and $\varepsilon_{d\,n}$ are the single-boson energies of the s- and d-bosons in the $2n$-th oscillator shell, etc. Furthermore, $\hat{N}_{s\,n} = s_n^\dagger s_n$ and $\hat{N}_{d\,n} = d_n^\dagger \cdot \tilde{d}_n$ are the number operators of the s- and d-bosons in the $2n$-th oscillator shell, respectively, and γ is the strength of the quadrupole-quadrupole interaction. In (1), the quadrupole operators are expressed as

$$\hat{Q}_M = \alpha \sum_{n=0}^{P-1} \left(d_{n+1\,M}^\dagger + \tilde{d}_{n+1\,M} \right) + \sum_{n=0}^{P} \left(d_{n\,M}^\dagger s_n + s_n^\dagger \tilde{d}_{n\,M} + \chi_n \left(d_n^\dagger \times \tilde{d}_n \right)_M^{(2)} \right) \tag{2}$$

with $-\sqrt{7}/2 \leq \chi_n \leq \sqrt{7}/2$, where $\tilde{d}_{2\,M} = (-1)^M d_{2-M}$, and α is a dimensionless parameter. It is obvious that this type of configuration mixing is induced by the 1p-1h type d-bosons in the first term of (2), which, however, is neglected in both the valence shell model calculation and the original IBM.

Note that the Hamiltonian (1) is exactly the general IBM Hamiltonian in the CQ formalism when it is confined to the $n = 0$ valence shell only with the E2 transition operator being $T_{2\,M}(E2) = q_2\, \hat{Q}_M$ if the first term in (2) is removed. Like the configuration mixing schemes with multiple 2p-2h excitations [5–8], the shape phase control parameters ($\varepsilon_{s\,n}$, $\varepsilon_{d\,n}$, χ_n) can also be taken as n-dependent which ultimately results in the addition of a shape coexistence feature to the theory. Moreover, the summations in (1) and (2) should run over all oscillator shells from the valence shell up to infinity as $P \to \infty$. It should be noted that the model Hamiltonian (1) without being able to distinguish bosons from different oscillator shells, or equivalently without the shell label n, is reduced to the hydrodynamic limit [16,17,24] of the symplectic collective model [15].

The Hamiltonian (1) is diagonalized in the U(6)⊃SU(3)⊃SO(3) basis for the s- and d-bosons in each oscillator shell with the basis vectors consecutively coupled at the SU(3) level as follows:

$$\left| \begin{array}{ccc} [N_0] & \cdots & [N_P] \\ (\lambda_0, \mu_0) & \cdots & (\lambda_P, \mu_P) \\ (\lambda_{0,1}, \mu_{0,1}) & \cdots & (\lambda_{0,P-1}, \mu_{0,P-1}) \\ & \rho(\lambda,\mu)\kappa\, L\, M & \end{array} \right\rangle =$$

$$\prod_{n=0}^{P-1} \sum_{\substack{\kappa_n L_n M_n \\ \kappa_{0,n+1} L_{0,n+1} M_{0,n+1}}}{}' \langle L_{0,n} M_{0,n}; L_{n+1} M_{n+1} | L_{0,n+1} M_{0,n+1} \rangle \langle i_{0,n}; i_{n+1} || \rho_{0,n+1} i_{0,n+1} \rangle |[N_0] i_0 M_0 \cdots [N_{P-1}] i_{P-1} M_{P-1}\rangle, \tag{3}$$

where P is the maximum number of $2\hbar\omega$ excitations included in the analysis, N_n counts the number of bosons in the n-th oscillator shell, $i_{0,n} \equiv \{(\lambda_{0,n}, \mu_{0,n}), \kappa_{0,n}, L_{0,n}, M_{0,n}\}$ and $i_{n+1} \equiv \{(\lambda_{n+1}, \mu_{n+1}), \kappa_{n+1}, L_{n+1}, M_{n+1}\}$, in which $\kappa_{0,n}$, κ_{n+1} are the branching multiplicity labels needed in the SU(3)⊃SO(3) reduction, with $(\lambda_{0,0}, \mu_{0,0}) \equiv (\lambda_0, \mu_0)$, $(\lambda_{0,P}, \mu_{0,P}) \equiv (\lambda, \mu)$, $\kappa_{0,0} \equiv \kappa_0$, $\kappa_{0,P} \equiv \kappa$, $L_{0,0} \equiv L_0$, $L_{0,P} \equiv L$, $M_{0,0} \equiv M_0$, and $M_{0,P} \equiv M$, the prime indicates that the quantum numbers κ, L, and M should be excluded in the summation, $\rho = \{\rho_{0,1}, \cdots, \rho_{0,P}\}$ is the set of the outer-multiplicity labels needed for the SU(3) coupling involved, $\langle L_{0,n} M_{0,n}; L_{n+1} M_{n+1} | L_{0,n+1} M_{0,n+1} \rangle$ is the SO(3) Clebsch-Gordan coefficient, and $\langle i_{0,n}; i_{n+1} || \rho_{0,n+1} i_{0,n+1} \rangle$ is the SU(3)⊃SO(3) Wigner coefficient, of which the computation code is available [25,26]. Reduced matrix elements of s- or d-boson creation and annihilation operators were provided in [27], which are necessary in the calculation.

3. Applications

As an application of the theory, the extended IBM Hamiltonian (1) is applied to fit level energies up to 3 MeV, experimentally known B(E2) values, electric quadrupole moments, and B(E0) values of the transitions among low-lying levels, and the isoscalar GMR and GQR of ^{152}Sm. In the original IBM calculation for ^{152}Sm, the Hamiltonian is diagonalized within $N_0 = 10$ subspace [28–30] equivalent to the shell model calculation confined within the $n = 0$ valence shell. In the present work, the calculation including $(N_0 = 10, N_1 = 0, N_2 = 0)$, $(N_0 = 10, N_1 = 1, N_2 = 0)$, $(N_0 = 10, N_1 = 2, N_2 = 0)$, and $(N_0 = 10, N_1 = 0, N_2 = 1)$ excitations up to $4\hbar\omega$ in excitation energy is performed. In the calculation, $\chi_n = -\sqrt{7}/2$ $\forall\, n$ is taken for simplicity. Besides the effective model parameters $\Delta_{ds} = \varepsilon_{d\,0} - \varepsilon_{s\,0}$ and γ, $\varepsilon_{d\,n}$ and $\varepsilon_{s\,n}$ for $n \geq 1$ are expressed as

$$\varepsilon_{s\,n} = \varepsilon_{s\,n}^{(0)} + 2\,n\,\hbar\omega, \quad \varepsilon_{d\,n} = \varepsilon_{d\,n}^{(0)} + 2\,n\,\hbar\omega \tag{4}$$

with $2\hbar\omega = 82\mathrm{A}^{-1/3}$ MeV = 15.365 MeV for ^{152}Sm. In the present calculation, Δ_{ds}, γ, $\varepsilon_{d\,2}^0 = \varepsilon_{d\,1}^0$, $\varepsilon_{s\,2}^0 = \varepsilon_{s\,1}^0$, and α are systematically adjusted according to the level energies, electric quadrupole moments of low-lying states, E0 and E2 transition rates, the isoscalar GMR and GQR strengths

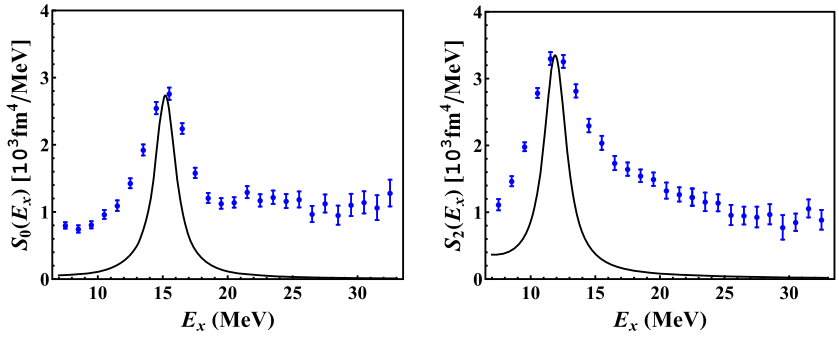

Fig. 1. The $\Lambda = 0$ and $\Lambda = 2$ strength distributions for ^{152}Sm, where the blue dots with error-bars are the experimental data provided by the author of [33] and the black solid curves are produced by the present model.

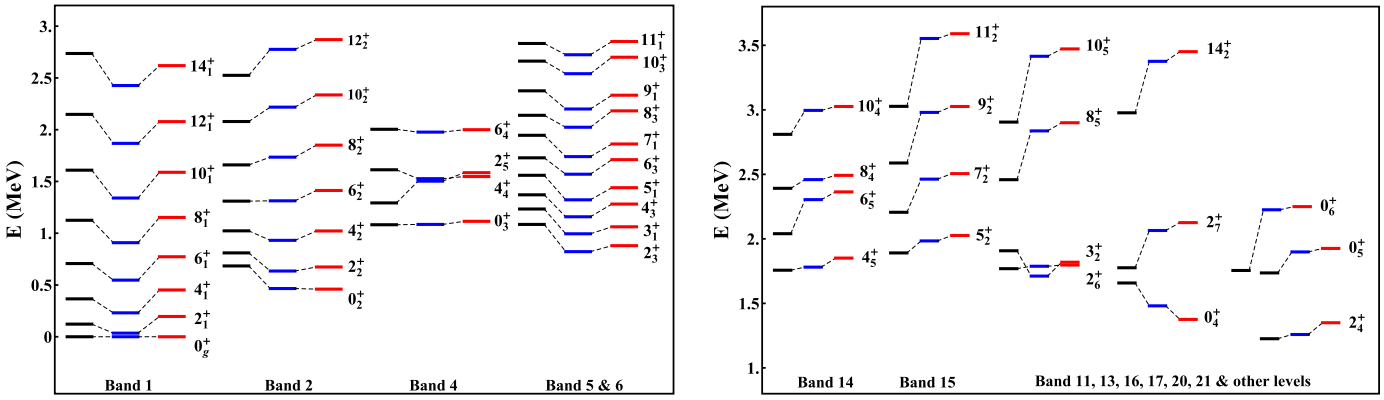

Fig. 2. Level energies (in MeV) of the 13 experimentally identified positive parity bands of ^{152}Sm, where the left (black) levels are those observed in experiments [34], the middle (blue) levels are those obtained from the present model, and the right (red) levels are those obtained from the original CQ formalism with $\Delta_{ds} = 0.457$ MeV, $\gamma = 0.011$ MeV, and $\chi = -\sqrt{7}/2$.

and distributions. The E0 transition operator is taken as $T(\mathrm{E0}) = \beta_0 \sum_{n=0}^{P} \hat{N}_{sn} + \beta \sum_{n=1}^{P} (s_n^\dagger + s_n)$, where β_0 is mainly determined by E0 transitions among low-lying states, while β is mainly determined by the isoscalar GMR. The E2 transition operators in the present model are taken as $T_{2\,M}(\mathrm{E2}) = q_2 \hat{Q}_M$ with the quadrupole operator $\hat{Q}_{2\,M}$ shown in (2), in which the parameter α is mainly determined by the isoscalar GQR. It is noted that for larger α values, smaller γ values are needed in order to fit the low-lying energy levels and the B(E2) transition rates, which implies that this kind of configuration mixing is deformation related. The EΛ transition strength as a function of the excitation energy E_x is defined as [31,32]

$$S_\Lambda(E_x) = \frac{\Gamma}{2\pi} \sum_\xi \frac{(2\Lambda+1)|\langle \xi;\Lambda||T(\mathrm{E}\Lambda)||0\rangle|^2}{(E_x - E_\xi)^2 + \frac{\Gamma^2}{4}}, \tag{5}$$

where $|0\rangle$ stands for the ground state, $|\xi;\Lambda\rangle$ is the excited state with angular momentum and parity Λ^+ and eigen-energy E_ξ, and a folding width of $\Gamma = 2$ MeV is used. The fitting to the experimental level energies and $\Lambda = 0$ and $\Lambda = 2$ strength functions of ^{152}Sm yields $\alpha = 3.30$, $\Delta_{ds} = 0.43$ MeV, $\gamma = 0.0135$ MeV, $\varepsilon^0_{s1} = -0.18$ MeV, and $\varepsilon^0_{d1} = -3.1$ MeV. During the fitting, the effective charge parameters q_2 and β_0 are fixed by B(E2, $2_1^+ \to 0_g^+$) and B(E0, $0_2^+ \to 0_g^+$), respectively, while β is determined by the isoscalar GMR strength, which yields $q_2 = 0.143$ eb, $\beta_0 = 0.054$ eb, and $\beta = 0.931$ eb. The centroid energy E_c defined by

$$E_c = \frac{\langle E_1\rangle}{\langle E_0\rangle}, \quad \langle E_k\rangle = \int_{E_a}^{E_b} E^k S_\Lambda(E)\,dE, \tag{6}$$

where $[E_a, E_b]$ is taken to be the values used in the experimental analysis [33]. The present model calculation yields $E_c^{\mathrm{GMR}} = 15.46$ MeV, which is near to the isoscalar GMR high energy peak position reported in [33], while $E_c^{\mathrm{GQR}} = 12.63$ MeV, which seems close to the average energy position of the low energy peak at 11.53 MeV with 71% EWSR and 14.86 MeV with 40% EWSR reported in [33]. As shown by the solid curves in Fig. 1, the peaks in the strength functions are well reproduced, but with insufficient width. This may be due to the fact that possible 2p-2h configuration mixing [5–8] is not considered, and only one type of boson excitations without distinction between neutrons and protons are included for the $2n$-th oscillator shell, which could also account for the fact that the model is unable to reproduce the low-energy peak in $S_0(E_x)$ and the high-energy peak in $S_2(E_x)$ [33].

Fig. 2 compares model predictions for energy levels to the experimentally determined values up to 3 MeV for 13 positive parity bands of ^{152}Sm. It should be noted that many levels classified as non-band-head excitations are not identified in the present calculation. The only exceptions to this are the 0_5^+ level at 1.736 MeV and the 2_4^+ level at 1.226 MeV that are shown in the right panel of Fig. 2, which are considered to be due to their excitation energies being lower than the excited levels with the same spin in the 13 bands, though they belong to non-band excitations. The level

Table 1
B(E2, $L_i \to L_f$) values (in W.u.), electric quadrupole moment $Q(L_\xi^+)$ (in eb), and $10^3\, B(\mathrm{E0}, 0_i^+ \to 0_f^+)/e^2R^4$ [given in the last row of the Table] of ^{152}Sm fitted by the present model and the CQ formalism, where the experimental $10^3\, B(\mathrm{E0}, 0_i^+ \to 0_f^+)/e^2R^4$ values are taken from [35], and * indicates that the corresponding value is fixed according to the experimental data.

	Exp. [34]	This work	CQ		Exp. [34]	This work	CQ		Exp. [34]	This work	CQ
$2_1^+ \to 0_g^+$	145 (16)	145*	145*	$2_6^+ \to 0_g^+$	$0.58^{0.16}_{-0.15}$	0.001	0.002	$2_6^+ \to 0_2^+$	$7.6^{2.2}_{-2.0}$	0.002	0.036
$4_1^+ \to 2_1^+$	209.5(22)	230.38	262.60	$4_2^+ \to 2_1^+$	0.74 (12)	0.13	0.20	$4_3^+ \to 2_2^+$	$0.3^{0.18}_{-0.13}$	1.61	0.71
$6_1^+ \to 4_1^+$	240(4)	254.55	320.43	$2_3^+ \to 2_1^+$	7.4 (10)	2.80	2.84	$2_3^+ \to 4_1^+$	0.56 (8)	5.11	35.34
$8_1^+ \to 6_1^+$	293(4)	258.14	345.49	$2_3^+ \to 0_g^+$	2.9 (4)	2.68	1.92	$4_2^+ \to 6_1^+$	17 (3)	13.67	20.13
$10_1^+ \to 8_1^+$	$314^{3.5}_{-2.6}$	251.88	346.85	$4_3^+ \to 2_1^+$	$0.7^{0.5}_{-0.3}$	0.86	0.70	$2_6^+ \to 4_3^+$	$40^{1.3}_{-1.2}$	14.95	21.65
$2_2^+ \to 0_2^+$	170 (12)	89.04	93.30	$3_1^+ \to 2_1^+$	$6.8^{1.5}_{-1.1}$	3.55	5.63	$4_2^+ \to 4_1^+$	$5.0^{1.0}_{-0.7}$	9.16	29.75
$4_2^+ \to 2_2^+$	250 (4)	148.83	157.65	$2_2^+ \to 0_g^+$	0.94 (6)	0.06	2.15	$4_3^+ \to 6_1^+$	$0.9^{0.6}_{-0.4}$	5.44	22.98
$3_1^+ \to 2_3^+$	120^{6}_{-9}	165.52	148.21	$0_3^+ \to 2_1^+$	$0.8^{0.53}_{-0.23}$	2.08	0.21	$2_2^+ \to 2_1^+$	5.7 (4)	11.70	51.64
$4_3^+ \to 2_3^+$	62^{35}_{-24}	68.61	120.26	$3_1^+ \to 4_1^+$	$7.2^{1.6}_{-1.1}$	3.95	13.33	$0_3^+ \to 2_2^+$	34^{23}_{-11}	129.95	130.97
$2_2^+ \to 4_1^+$	18 (12)	22.14	42.76	$4_3^+ \to 4_1^+$	7^{4}_{-3}	1.89	1.96	$0_2^+ \to 2_1^+$	33.3 (12)	85.48	224.52
$Q(2_1^+)$	-1.683 (18)	-1.769	-1.758	$Q(4_1^+)$	-2.6 (14)	-2.319	-2.469				
$0_2^+ \to 0_g^+$	51 (5)	51*	51*	$0_3^+ \to 0_g^+$	0.7 (4)	2.26	0.016	$0_3^+ \to 0_2^+$	23 (9)	56.83	1.0

Table 2
(N_0, N_1, N_2) configuration contribution to the excited states of ^{152}Sm in the present model.

Configuration	0_g^+	2_1^+	4_1^+	6_1^+	8_1^+	0_2^+	0_3^+	2_2^+	2_3^+	2_4^+	2_5^+
$(N_0, N_1 = 0, N_2 = 0)$	0.996231	0.989017	0.988679	0.993224	0.993333	0.997152	0.997020	0.992098	0.992698	0.992592	0.992643
$(N_0, N_1 = 1, N_2 = 0)$	0.003657	0.010553	0.010906	0.006562	0.006454	0.002746	0.002875	0.007540	0.007019	0.007085	0.007041
$(N_0, N_1 = 2, N_2 = 0)$	0.000111	0.000428	0.000414	0.000214	0.000213	0.000101	0.000104	0.000361	0.000282	0.000322	0.000314
$(N_0, N_1 = 0, N_2 = 1)$	1.0×10^{-6}	2.0×10^{-6}	1.0×10^{-6}	≈ 0	≈ 0	1.0×10^{-6}	1.0×10^{-6}	1.0×10^{-6}	1.0×10^{-6}	1.0×10^{-6}	2.0×10^{-6}

pattern produced by the present model follows the experimental data. The original CQ formalism confined in the $N_0 = 10$ subspace with $\alpha = 0$, $\Delta_{ds} = 0.457$ MeV, $\gamma = 0.011$ MeV are also shown for comparison. It is clearly shown in Fig. 2 that levels in Band 1, 2, 5, and 6, especially those low-lying ones, are well fit by the original CQ formalism, but levels in other bands, especially those high-lying ones, are fitted slightly better by the present model. For the 46 excited levels fitted, the root-mean-square deviation for the level energies in the present model is 0.23 MeV, while it is 0.24 MeV in the original CQ formalism, suggesting that the multiple $2\hbar\omega$ excitations of the type introduced herein are slightly better in describing all excited levels up to 3 MeV.

Table 1 compares results from the present model to the experimentally known B(E2) values, electric quadrupole moments, and $B(\mathrm{E0})/e^2R^4$ values of ^{152}Sm, where R is the radius of ^{152}Sm. It is shown that most intra-band and inter-band transitions follow the experimental data patten, except for B(E2, $0_2^+ \to 2_1^+$) and B(E2, $0_3^+ \to 2_2^+$), which are 2.57 and 3.82 times larger than the corresponding experimental values, respectively. The root-mean-square deviation for the B(E2) values is 30.18 W.u. and 36.47 W.u. in the present model and the original CQ formalism, respectively, when B(E2, $0_2^+ \to 2_1^+$) and B(E2, $0_3^+ \to 2_2^+$) are excluded, while it is 35.32 W.u. and 52.66 W.u when all B(E2) values shown in Table 1 are included. The large deviation in fitting to these two B(E2) values, especially when levels in the 13 bands up to 3 MeV are all considered in a fit, may be due to the fact that 0_2^+, 0_3^+, and possibly other low-lying states are strongly mixed with intruder states resulting from neutron 2p-2h excitations from below the valence shell [9,36]. Anyway, as far as the level energies and the B(E2) values are concerned, the fitting results of the present model are noticeably better than those of the original CQ formalism indicating the multiple $2\hbar\omega$ excitations of the type introduced are of importance not only in describing the isoscalar GMR and GQR phenomena, but also in describing low-energy structural properties of ^{152}Sm. Furthermore, it is worthy to note that the effective charge parameter used in the CQ formalism is $q_2 = 0.182$ eb, which is larger than that used in the present model with $q_2 = 0.143$ eb, indicating that the effective charge is reduced due to the multiple $2\hbar\omega$ excitations introduced.

Table 2 provides (N_0, N_1, N_2) configuration contribution to the excited states defined by

$$v(N_0, N_1, N_2, L_\xi) = \sum_\eta |\langle [N_0], [N_1], [N_2], \eta, L | L_\xi \rangle|^2, \tag{7}$$

where η stands for all the additional quantum number needed, $|L_\xi\rangle$ is the ξ-th excited state of the model with angular momentum quantum number L, and $|[N_0], [N_1], [N_2], \eta, L\rangle$ is the SU(3) coupled basis vectors with $N_1 = 0, 1, 2$ and $N_2 = 0, 1$ shown in (3). It is clearly shown that $(N_0, N_1 = 0, N_2 = 0)$ configuration always dominates in the excited states of the model. Most notably, there is 0.7 – 1% contribution from $(N_0, N_1 = 1, N_2 = 0)$ configuration to the 2_ξ^+ states with $\xi \le 5$ and 4_1^+ state due to the configuration mixing term in the quadrupole operators introduced, while $(N_0, N_1 = 0, N_2 = 1)$ configuration can be neglected. Generally speaking, the configuration mixing improves theoretical B(E2) values except for B(E2, $10_1^+ \to 8_1^+$) and B(E2, $3_1^+ \to 2_3^+$), of which the results of the CQ formalism are obviously better.

4. Conclusions

In summary, a multi-shell extension of the IBM for even-even nuclei that includes multiple $2\hbar\omega$ excitations is proposed by using the general quadrupole operators involving multi-shell mixing with the next nearest same parity oscillator shell as suggested by the successes of the Sp(3, **R**) collective and no-core shell model studies. As a first test of this $2\hbar\omega$ 1p-1h mixing concept within an IBM framework, an extended CQ-IBM Hamiltonian was applied to level energies up to 3 MeV, experimentally known B(E2) values, electric quadrupole moments, and B(E0) values among low-lying levels that reflect couplings to the isoscalar GMR and GQR of ^{152}Sm. The results show that while the low-lying spectral properties of ^{152}Sm [28–30] are reasonably well described within the framework of the non-extended CQ-IBM formalism up to about 3 MeV, they are even better described in the extended CQ formalism, with only a few exceptions for intra-band transitions. Hence it seems that the multiple $2\hbar\omega$ excitations are

not only of importance in describing both low-lying and highly excited levels, but also indispensable for elucidating the importance of including isoscalar GMR and GQR phenomena in such analyses.

However, deviation in fitting B(E2, $0_2^+ \to 2_1^+$) and B(E2, $0_3^+ \to 2_2^+$) by the present model is still large, which is possibly related to the long term debate on the nature of the low-lying 0^+ states in these deformed nuclei [36,37]. Due to the large deformation, neutron 2p-2h excitations from below the valence shell are likely to occur in ^{152}Sm [9,37]. Moreover, the present model can not reproduce the widely populated isoscalar GMR and GQR strengths with several peaks. Besides the multiple 2p-2h configuration mixing [5–8], which is not only necessary to improve theoretical B(E2) values of the transitions among low-lying levels, but also possible to improve the description of the isoscalar GMR and GQR distributions, similar extension of the IBM-II with both neutron and proton types of s and d bosons in the $2\hbar\omega$ shell seems also necessary, which are worthy to be further analyzed.

Declaration of competing interest

The authors declare that they have no known competing financial interests or personal relationships that could have appeared to influence the work reported in this paper.

Data availability

Data will be made available on request.

Acknowledgements

The authors are very much grateful to Professor M. Itoh from Tohoku University, Japan for providing their experimental data of the isoscalar GMR and GQR strength distributions of ^{152}Sm. One of the authors (F. P.) is grateful to Professor Yi-Fei Niu from Lanzhou Univ., China for enlightening discussions on the GMR and GQR phenomena. Support from the National Natural Science Foundation of China (12175097, 12175066) and from LSU through its Sponsored Research Rebate Program as well as under the LSU Foundation's Distinguished Research Professorship Program is acknowledged.

Appendix A. Matrix elements in the SU(3) coupled basis

The reduced matrix elements of the number operator $\hat{N}_{sn}$ are given by

$$\begin{aligned}&\left\langle [N_n](\lambda_n'\mu_n')[N_m](\lambda_m'\mu_m'); f \middle| \hat{N}_{sn} \middle| [N_n](\lambda_n\mu_n)[N_m](\lambda_m\mu_m); i \right\rangle \\ &= \sum_{\substack{\kappa_n,L_n,\kappa_m,L_m,\\ \kappa_n',L_n',\kappa_m',L_m'}} \langle i_n;i_m||i\rangle \langle f_n;f_m||f\rangle \langle [N_n]f_n|| \hat{N}_{sn} ||[N_n]i_n\rangle \delta_{\lambda_m',\lambda_m}\delta_{\mu_m',\mu_m},\end{aligned} \tag{A.1}$$

where $|i\rangle = |(\lambda,\mu)\kappa L\rangle$ and $|f\rangle = \left|(\lambda',\mu')\kappa' L'\right\rangle$, $\langle i_n;i_m||i\rangle$ and $\langle f_n;f_m||f\rangle$ are the Wigner coefficients of SU(3)⊃ SO(3) provided in [25,26], and

$$\langle [N_n]f_n|| \hat{N}_{sn} ||[N_n]i_n\rangle = \sum_{g_n} \langle [N_n]f_n|| s_n^\dagger ||[N_n-1]g_n\rangle \langle [N_n-1]g_n|| s_n ||[N_n]i_n\rangle, \tag{A.2}$$

in which the SU(3) reduced matrix elements of s-boson creation and annihilation operators were provided in [27].

Since only $(N_0=10,N_1=0,N_2=0)$, $(N_0=10,N_1=1,N_2=0)$, $(N_0=10,N_1=2,N_2=0)$, and $(N_0=10,N_1=0,N_2=1)$ configurations are considered, $\hat{Q}\cdot\hat{Q}$ in (1) for this case can be expressed effectively as

$$\begin{aligned}&\hat{Q}\cdot\hat{Q} = 10\alpha^2 + 2\alpha^2\textstyle\sum_{m=1}^2 \hat{N}_m - 2\alpha^2\sum_{m=1}^2 \hat{N}_{sm} + \hat{Q}_c\cdot\hat{Q}_c + \alpha^2(d_1^\dagger\cdot\tilde{d}_1^\dagger + \tilde{d}_1\cdot\tilde{d}_1) + \\ &2\alpha^2(d_1^\dagger\cdot\tilde{d}_2 + d_2^\dagger\cdot\tilde{d}_1) + \alpha\textstyle\sum_{m=1}^2(d_m^\dagger+\tilde{d}_m)\cdot\hat{Q}_c + \alpha\sum_{m=1}^2\hat{Q}_c\cdot(d_m^\dagger+\tilde{d}_m),\end{aligned} \tag{A.3}$$

where $\hat{Q}_{c\,M} = \sum_i \hat{Q}_M(i)$, in which $\hat{Q}_{2\,M}(i) = (d_{i\,M}^\dagger s_i + s_i^\dagger \tilde{d}_{i\,M}) - \frac{\sqrt{7}}{2}\left(d_i^\dagger\times\tilde{d}_i\right)_M^{(2)}$ are generators of SU(3) used in this work, and the relation $\hat{N}_m = \hat{N}_{dm} + \hat{N}_{sm}$ is used in (A.3).

Matrix elements of $\sum_{m=1}^2 \hat{N}_m$ in (A.3) can easily be read out for given $[N_1]$ and $[N_2]$ in the coupled basis (3), while the matrix elements of $\hat{N}_{sm}$ in (A.3) are given by (A.1). In the IBM, $C_2(SU(3)) = 2\,\hat{Q}_c\cdot\hat{Q}_c + \frac{3}{4}L\cdot L$, where $C_2(SU(3))$ is the Casimir operator of SU(3). Hence, we have

$$\begin{aligned}&\left\langle \begin{matrix}[N_0] & [N_m'] & (\lambda',\mu')\\ (\lambda_0',\mu_0') & (\lambda_m',\mu_m'); & \kappa'\,L\,M\end{matrix} \middle| \hat{Q}_c\cdot\hat{Q}_c \middle| \begin{matrix}[N_0] & [N_m] & (\lambda,\mu)\\ (\lambda_0,\mu_0)(\lambda_m,\mu_m); & \kappa\,L\,M\end{matrix} \right\rangle = \\ &\delta_{(\lambda_0'\mu_0')(\lambda_0\mu_0)}\delta_{(\lambda_m'\mu_m')(\lambda_m\mu_m)}\delta_{\kappa',\kappa}\delta_{(\lambda'\mu')(\lambda\mu)}\left(\tfrac{1}{2}(\lambda^2+\mu^2+\lambda\mu+3\lambda+3\mu) - \tfrac{3}{8}L(L+1)\right).\end{aligned} \tag{A.4}$$

For $[N_m'] = [1]$ or $[2]$ with $m=1$ or 2, the SU(3) couplings involved are outer multiplicity-free, so the outer multiplicity labels are omitted in the following. Using the Wigner-Racah calculus, one obtains

$$\begin{aligned}&\left\langle \begin{matrix}[N_0] & [N_m] & (\lambda,\mu)\\ (\lambda_0,\mu_0) & (\lambda_m,\mu_m); & \kappa\,L\,M\end{matrix} \middle| \hat{Q}_c\cdot\tilde{d}_m \middle| \begin{matrix}[N_0] & [N_m'] & (\lambda',\mu')\\ (\lambda_0',\mu_0')(\lambda_m',\mu_m'); & \kappa'\,L\,M\end{matrix} \right\rangle = \\ &\left\langle \begin{matrix}[N_0] & [N_m'] & (\lambda',\mu')\\ (\lambda_0',\mu_0') & (\lambda_m',\mu_m'); & \kappa'\,L\,M\end{matrix} \middle| d_m^\dagger\cdot\hat{Q}_c \middle| \begin{matrix}[N_0] & [N_m] & (\lambda,\mu)\\ (\lambda_0,\mu_0)(\lambda_m,\mu_m); & \kappa\,L\,M\end{matrix} \right\rangle = \delta_{(\lambda_0'\mu_0')(\lambda_0\mu_0)}\times \\ &\delta_{N_m',N_m+1}\sqrt{N_m+1}\left\langle \begin{matrix}[N_m] & [1]\\ (\lambda_m,\mu_m) & (2,0)\end{matrix} \middle| \begin{matrix}[N_m']\\ (\lambda_m',\mu_m')\end{matrix} \right\rangle [\tfrac{1}{2}(\lambda^2+\mu^2+\lambda\mu+3\lambda+3\mu)]^{\frac{1}{2}}(-1)^{\phi_\mu}\times\end{aligned}$$

$$\sum_{\tilde{\kappa},\tilde{L},\kappa_0',L_0',\kappa_1',L_1',\tilde{\kappa}_1,\tilde{L}_1}\left\langle(\lambda_0',\mu_0')\kappa_0'\,L_0';(\lambda_m',\mu_m')\kappa_1'L_1'\|(\lambda',\mu')\kappa'L\right\rangle\left\langle(\lambda_0',\mu_0')\kappa_0'\,L_0';(\lambda_m,\mu_m)\tilde{\kappa}_1\,\tilde{L}_1\|(\lambda,\mu)\,\tilde{\kappa}\,\tilde{L}\right\rangle\times$$
$$\left\langle(\lambda_m,\mu_m)\,\tilde{\kappa}_1\,\tilde{L}_1;(2,0)\,1\,2\|(\lambda_m',\mu_m')\,\kappa_1'\;\;L_1'\right\rangle\left\langle(\lambda,\mu)\,\kappa\,L;(1,1)1\,2\|(\lambda,\mu)\rho''=1\,\tilde{\kappa}\,\tilde{L}\right\rangle\times$$
$$(-1)^{L_0'+\tilde{L}+\tilde{L}_1}(2\tilde{L}+1)\sqrt{(2L_1'+1)/(2L+1)}\left\{\begin{array}{ccc}L_0' & L_1' & L\\ 2 & \tilde{L} & \tilde{L}_1\end{array}\right\},\tag{A.5}$$

$$\left\langle\begin{array}{ccc}[N_0] & [N_m'] & (\lambda',\mu')\\ (\lambda_0',\mu_0') & (\lambda_m',\mu_m'); & \kappa'\,L\,M\end{array}\right|\hat{Q}_c\cdot d_m^{\dagger}\left|\begin{array}{ccc}[N_0] & [N_m] & (\lambda,\mu)\\ (\lambda_0,\mu_0)(\lambda_m,\mu_m); & \kappa\,L\,M\end{array}\right\rangle=$$
$$\left\langle\begin{array}{ccc}[N_0] & [N_m] & (\lambda,\mu)\\ (\lambda_0,\mu_0) & (\lambda_m,\mu_m); & \kappa\,L\,M\end{array}\right|\tilde{d}_m\cdot\hat{Q}_c\left|\begin{array}{ccc}[N_0] & [N_m'] & (\lambda',\mu')\\ (\lambda'_0,\mu'_0)(\lambda_m',\mu_m'); & \kappa'\,L\,M\end{array}\right\rangle=\delta_{(\lambda_0'\mu_0')(\lambda_0\mu_0)}\times$$
$$\delta_{N_m',N_m+1}\sqrt{N_m+1}\left\langle\begin{array}{ccc}[N_m] & [1] & \\ (\lambda_m,\mu_m) & (2,0) & \end{array}\right|\left.\begin{array}{c}[N_m']\\ (\lambda_m',\mu_m')\end{array}\right\rangle[\tfrac{1}{2}(\lambda'^2+\mu'^2+\lambda'\mu'+3\lambda'+3\mu')]^{\frac{1}{2}}(-1)^{\phi_{\mu'}}\times$$
$$\sum_{\tilde{\kappa},\tilde{L},\kappa_0,L_0,\kappa_1',L_1',\kappa_1,L_1}\left\langle(\lambda_0',\mu_0')\kappa_0\,L_0;(\lambda_m',\mu_m')\kappa_1'L_1'\|(\lambda',\mu')\,\tilde{\kappa}\,\tilde{L}\right\rangle\langle(\lambda_0,\mu_0)\kappa_0\,L_0;(\lambda_m,\mu_m)\,\kappa_1\,L_1\|(\lambda,\mu)\,\kappa\,L\rangle\times$$
$$\left\langle(\lambda_m,\mu_m)\,\kappa_1\,L_1;(2,0)\,1\,2\|(\lambda_m',\mu_m')\,\kappa_1'\;\;L_1'\right\rangle\left\langle(\lambda',\mu')\,\tilde{\kappa}\,\tilde{L};(1,1)\,1\,2\|(\lambda',\mu')\rho''=1\,\kappa'\,L\right\rangle\times$$
$$(-1)^{L_0+L-L_1}\sqrt{(2L_1'+1)(2\tilde{L}+1)}\left\{\begin{array}{ccc}L_0 & L_1' & \tilde{L}\\ 2 & L & L_1\end{array}\right\},\tag{A.6}$$

where

$$\left\langle\begin{array}{ccc}[N_0] & [N_m'] & (\lambda',\mu')\\ (\lambda_0',\mu_0') & (\lambda_m',\mu_m'); & \kappa'\,L'\end{array}\right\|\hat{Q}_c\left\|\begin{array}{ccc}[N_0] & [N_m] & (\lambda,\mu)\\ (\lambda_0,\mu_0)(\lambda_m,\mu_m); & \kappa\,L\end{array}\right\rangle=$$
$$\delta_{(\lambda_0'\mu_0')(\lambda_0\mu_0)}\delta_{(\lambda_m'\mu_m')(\lambda_m\mu_m)}\delta_{(\lambda'\mu')(\lambda\mu)}\langle(\lambda,\mu)\,\kappa\,L;(1,1)\,1\,2\|(\lambda,\mu)\,\rho'=1\,\kappa'\,L'\rangle\times$$
$$[\tfrac{1}{2}(\lambda^2+\mu^2+\lambda\mu+3\lambda+3\mu)]^{\frac{1}{2}}(-1)^{\phi_\mu}\tag{A.7}$$

with $\phi_\mu=1-\delta_{\mu 0}$ is used [25,26],

$$\left\langle\begin{array}{ccc}[N_0] & [N_m'] & (\lambda',\mu')\\ (\lambda_0',\mu_0') & (\lambda_m',\mu_m'); & \kappa'\,L\,M\end{array}\right|d_m^{\dagger}\cdot d_m^{\dagger}\left|\begin{array}{ccc}[N_0] & [N_m] & (\lambda,\mu)\\ (\lambda_0,\mu_0)(\lambda_m,\mu_m); & \kappa\,L\,M\end{array}\right\rangle=$$
$$\left\langle\begin{array}{ccc}[N_0] & [N_m] & (\lambda,\mu)\\ (\lambda_0,\mu_0) & (\lambda_m,\mu_m); & \kappa\,L\,M\end{array}\right|\tilde{d}_m\cdot\tilde{d}_m\left|\begin{array}{ccc}[N_0] & [N_m] & (\lambda,\mu)\\ (\lambda'_0,\mu'_0)(\lambda_m',\mu_m'); & \kappa'\,L\,M\end{array}\right\rangle=\delta_{(\lambda_0'\mu_0')(\lambda_0\mu_0)}\times$$
$$\delta_{N_m',N_m+2}\sqrt{(N_m+1)(N_m+2)}\sum_{\tilde{\lambda}_m,\tilde{\mu}_m}\left\langle\begin{array}{ccc}[N_m] & [1] & \\ (\lambda_m,\mu_m) & (2,0) & \end{array}\right|\left.\begin{array}{c}[N_m+1]\\ (\tilde{\lambda}_m,\tilde{\mu}_m)\end{array}\right\rangle\left\langle\begin{array}{ccc}[N_m+1] & [1] & \\ (\tilde{\lambda}_m,\tilde{\mu}_m) & (2,0) & \end{array}\right|\left.\begin{array}{c}[N_m+2]\\ (\lambda_m',\mu_m')\end{array}\right\rangle$$
$$\sum_{\tilde{\kappa}_1,\tilde{L}_1,\kappa_0,L_0,\kappa_1,L_1,\kappa_1',L_1'}\left\langle(\lambda_0,\mu_0)\,\kappa_0\,L_0;(\lambda_m',\mu_m')\kappa_1'L_1'\|(\lambda',\mu')\,\kappa'L\right\rangle\langle(\lambda_0,\mu_0)\,\kappa_0\,L_0;(\lambda_m,\mu_m)\,\kappa_1\,L_1\|(\lambda,\mu)\,\kappa\,L\rangle\times$$
$$\left\langle(\tilde{\lambda}_m,\tilde{\mu}_m)\,\tilde{\kappa}_1\,\tilde{L}_1;(2,0)\,1\,2\|(\lambda_m',\mu_m')\,\kappa_1'\,L_1'\right\rangle\left\langle(\lambda_m,\mu_m)\,\kappa_1\,L_1;(2,0)\,1\,2\|(\tilde{\lambda}_m,\tilde{\mu}_m)\,\tilde{\kappa}_1\,\tilde{L}_1\right\rangle,\tag{A.8}$$

$$\left\langle\begin{array}{ccc}[N_0] & [N_1'] & [N_2']\\ (\lambda_0',\mu_0') & (\lambda_1',\mu_1') & (\lambda_2',\mu_2')\\ (\lambda_{01}',\mu_{01}') & (\lambda',\mu'); & \kappa'\,L\,M\end{array}\right|d_1^{\dagger}\cdot\tilde{d}_2\left|\begin{array}{ccc}[N_0] & [N_1] & [N_2]\\ (\lambda_0,\mu_0)(\lambda_1,\mu_1) & (\lambda_2,\mu_2) & \\ (\lambda_{01},\mu_{01}) & (\lambda,\mu); & \kappa\,L\,M\end{array}\right\rangle=$$
$$\left\langle\begin{array}{ccc}[N_0] & [N_1] & [N_2]\\ (\lambda_0,\mu_0) & (\lambda_1,\mu_1) & (\lambda_2,\mu_2)\\ (\lambda_{01},\mu_{01}) & (\lambda,\mu); & \kappa\,L\,M\end{array}\right|d_2^{\dagger}\cdot\tilde{d}_1\left|\begin{array}{ccc}[N_0] & [N_1] & [N_2]\\ (\lambda'_0,\mu'_0)(\lambda_1',\mu_1') & (\lambda_2',\mu_2') & \\ (\lambda'_{01},\mu'_{01}) & (\lambda',\mu'); & \kappa'\,L\,M\end{array}\right\rangle=\delta_{(\lambda_0'\mu_0')(\lambda_0\mu_0)}\times$$
$$\sum_{\kappa_0,L_0,\kappa_1',L_1',\kappa_{01}',L_{01}',\kappa_2',L_2'}\sum_{\kappa_1,L_1,\kappa_{01},L_{01},\kappa_2,L_2}\left\langle(\lambda_0,\mu_0)\,\kappa_0\,L_0;(\lambda_1',\mu_1')\kappa_1'L_1'\|(\lambda_{01}',\mu_{01}')\,\kappa_{01}'L_{01}'\right\rangle\times$$
$$\langle(\lambda_0,\mu_0)\,\kappa_0\,L_0;(\lambda_1,\mu_1)\,\kappa_1\,L_1\|(\lambda_{01},\mu_{01})\,\kappa_{01}\,L_{01}\rangle\times$$
$$\left\langle(\lambda_{01}',\mu_{01}')\,\kappa_{01}'\,L_{01}';(\lambda_2',\mu_2')\,\kappa_2'\,L_2'\|(\lambda',\mu')\,\kappa'\,L'\right\rangle\langle(\lambda_{01},\mu_{01})\,\kappa_{01}\,L_{01};(\lambda_2,\mu_2)\,\kappa_2\,L_2\|(\lambda,\mu)\,\kappa\,L\rangle\times$$
$$(-1)^{L_{01}+L_{01}'+L_0+L_1+L_2+L}\sqrt{(2L_{01}'+1)(2L_{01}+1)(2L_1+1)(2L_2+1)^2/(2L_2'+1)}\left\{\begin{array}{ccc}L_{01} & L_2 & L\\ L_2' & L_{01}' & 2\end{array}\right\}\left\{\begin{array}{ccc}L_{01}' & L_0 & L_1'\\ L_1 & 2 & L_{01}\end{array}\right\}\times$$
$$\left\langle N_1'(\lambda_1',\mu_1')\kappa_1'L_1'\right||\,d_1^{\dagger}\,|\left|N_1(\lambda_1,\mu_1)\kappa_1L_1\right\rangle\left\langle N_2(\lambda_2,\mu_2)\kappa_2L_2\right||\,d_2^{\dagger}\,|\left|N_2'(\lambda_2',\mu_2')\kappa_2'L_2'\right\rangle,\tag{A.9}$$

where

$$\langle N'(\lambda',\mu')\kappa'L'\|\hat{T}_l^{(2,0)}\|N(\lambda,\mu)\kappa L\rangle=\sqrt{N+1}\delta_{N',N+1}\times$$
$$\left\langle\begin{array}{ccc}[N] & [1] & \\ (\lambda,\mu) & (2,0) & \end{array}\right|\left.\begin{array}{c}[N']\\ (\lambda',\mu')\end{array}\right\rangle\left\langle(\lambda,\mu)\,\kappa\,L;(2,0)\,1\,l\|(\lambda',\mu')\,\kappa_1'\;\;L_1'\right\rangle\tag{A.10}$$

for $l=0$ or 2, in which $\hat{T}^{(2,0)}_{2\,M}=d^{\dagger}_M$ and $\hat{T}^{(2,0)}_0=s^{\dagger}$. In all the expressions shown above, $\left\langle\begin{array}{ccc}[N] & [1] & \\ (\lambda,\mu) & (2,0) & \end{array}\right|\left.\begin{array}{c}[N+1]\\ (\tilde{\lambda},\tilde{\mu})\end{array}\right\rangle$ *etc.* are the Wigner coefficients of U(6) ⊃ SU(3), which can be deduced from the analytical matrix elements of s- or d-boson creation operator shown in [27]. Similarly, one can derive that

$$\left\langle \begin{array}{ccc} [N_0] & [N'_m] & (\lambda',\mu') \\ (\lambda'_0,\mu'_0) & (\lambda'_m,\mu'_m); & \kappa' L' \end{array} \middle\| \hat{T}^{(2,0)}_l(m) \middle\| \begin{array}{ccc} [N_0] & [N_m] & (\lambda,\mu) \\ (\lambda_0,\mu_0) & (\lambda_m,\mu_m); & \kappa L \end{array} \right\rangle = \sqrt{N_m+1}\,\delta_{N'_m,N_m+1}\,\delta_{(\lambda'_0\mu'_0)(\lambda_0\mu_0)} \times$$
$$\sum_{\kappa'_0,L'_0,\kappa'_1,L'_1,\kappa_1,L_1} \left\langle (\lambda'_0,\mu'_0)\,\kappa'_0\,L'_0;(\lambda'_m,\mu'_m)\,\kappa'_1\,L'_1 \| (\lambda',\mu')\,\kappa'\,L' \right\rangle \left\langle (\lambda'_0,\mu'_0)\,\kappa'_0\,L'_0;(\lambda_m,\mu_m)\,\kappa_1\,L_1 \| (\lambda,\mu)\,\kappa\,L \right\rangle \times$$
$$\left\langle \begin{array}{ccc} [N_m] & [1] & \\ (\lambda_m,\mu_m) & (2,0) & \end{array} \middle| \begin{array}{c} [N'_m] \\ (\lambda'_m,\mu'_m) \end{array} \right\rangle \left\langle (\lambda_m,\mu_m)\,\kappa_1\,L_1;(2,0)\,1\,l \| (\lambda'_m,\mu'_m)\,\kappa'_1\;\; L'_1 \right\rangle \times$$
$$(-1)^{L'_0-L'-L_1}\sqrt{(2L'_1+1)(2L+1)} \left\{ \begin{array}{ccc} L'_0 & L'_1 & L' \\ l & L & L_1 \end{array} \right\}, \tag{A.11}$$

which is useful in calculating B(E2) values.

Finally, B(E2; $L_\xi \to L'_{\xi'}$) and electric quadrupole moment $Q(L_\xi)$ are given by

$$\mathrm{B(E2};\, L_\xi \to L'_{\xi'}) = (q_2)^2\,\frac{2L'+1}{2L+1}\,|\langle L'_{\xi'}||\hat{Q}||L_\xi\rangle|^2 \tag{A.12}$$

and

$$Q(L_\xi) = \sqrt{\tfrac{16\pi}{5}}\,q_2\langle LL;\,20|LL\rangle\langle L_\xi||Q||L_\xi\rangle, \tag{A.13}$$

respectively, because the SO(3) reduced matrix element used in this work is defined in terms of the SO(3) Clebsch-Gordan coefficient.

References

[1] A. Bohr, B.R. Mottelson, Nuclear Structure, vol. II: Nuclear Deformation, W. A. Benjamin, Reading, Massachusetts, USA, 1975.
[2] F. Iachello, A. Arima, The Interacting Boson Model, Cambridge University Press, Cambridge, UK, 1987.
[3] D. Bonatsos, Interacting Boson Models of Nuclear Structure, Oxford University Press, Oxford, UK, 1988.
[4] W. Pfeifer, An Introduction to the Interacting Boson Model of the Atomic Nucleus, vdf Hochschulverlag an der ETH, Zürich, Swizerland, 1998.
[5] P.D. Duval, B.R. Barrett, Configuration mixing in the interacting boson model, Phys. Lett. B 100 (1981) 223.
[6] P.D. Duval, B.R. Barrett, Quantitative description of configuration mixing in the interacting boson model, Nucl. Phys. A 376 (1982) 213.
[7] K. Heyde, P. Van Isacker, M. Waroquier, J.L. Wood, R.A. Meyer, Coexistence in odd-mass nuclei, Phys. Rep. 102 (1983) 291.
[8] J.L. Wood, K. Heyde, W. Nazarewicz, M. Huyse, P. Van Duppen, Coexistence in even-mass nuclei, Phys. Rep. 215 (1992) 101.
[9] K. Heyde, J.L. Wood, Shape coexistence in atomic nuclei, Rev. Mod. Phys. 83 (2011) 1467.
[10] J.P. Elliott, Collective motion in the nuclear shell model. I. Classification schemes for states of mixed configurations, Proc. R. Soc. Lond. A 245 (1958) 128.
[11] O. Castaños, J.P. Draayer, Y. Leschber, Quantum rotor and its SU(3) realization, Comput. Phys. Commun. 52 (1988) 71.
[12] G. Gneuss, U. Mosel, W. Greiner, A new treatment of the collective nuclear Hamiltonian, Phys. Lett. B 30 (1969) 397.
[13] G. Gneuss, U. Mosel, W. Greiner, On the relationship between the level-structures in spherical and deformed nuclei, Phys. Lett. B 31 (1970) 269.
[14] G. Gneuss, W. Greiner, Collective potential energy surfaces and nuclear structure, Nucl. Phys. A 171 (1971) 449.
[15] G. Rosensteel, D.J. Rowe, Nuclear Sp(3, R) model, Phys. Rev. Lett. 38 (1977) 10.
[16] G. Rosensteel, D.J. Rowe, u(3)-boson model of nuclear collective motion, Phys. Rev. Lett. 47 (1981) 223.
[17] D.J. Rowe, G. Rosensteel, Rotational bands in the u(3)-boson model, Phys. Rev. C 25 (1982) 3236.
[18] D.J. Rowe, Microscopic theory of the nuclear collective model, Rep. Prog. Phys. 48 (1985) 1419.
[19] G. Rosensteel, J.P. Draayer, K.J. Weeks, Symplectic shell-model calculation for ^{24}Mg, Nucl. Phys. A 419 (1984) 1.
[20] K.D. Launey, T. Dytrych, J.P. Draayer, Symmetry-guided large-scale shell-model theory, Prog. Part. Nucl. Phys. 89 (2016) 101–136.
[21] T. Dytrych, K.D. Sviratcheva, C. Bahri, J.P. Draayer, J.P. Vary, Evidence for symplectic symmetry in ab initio no-core shell model results for light nuclei, Phys. Rev. Lett. 98 (2007) 162503.
[22] T. Dytrych, K.D. Launey, J.P. Draayer, P. Maris, J.P. Vary, E. Saule, U. Catalyurek, M. Sosonkina, D. Langr, M.A. Caprio, Collective modes in light nuclei from first principles, Phys. Rev. Lett. 111 (2013) 252501.
[23] T. Dytrych, K.D. Launey, J.P. Draayer, D.J. Rowe, J.L. Wood, G. Rosensteel, C. Bahri, D. Langr, R.B. Baker, Physics of nuclei: key role of an emergent symmetry, Phys. Rev. Lett. 124 (2020) 042501.
[24] R. Le Blanc, J. Carvalho, D.J. Rowe, A coupled rotor-vibrator model as the macroscopic limit of the microscopic symplectic model, Phys. Lett. B 140 (1984) 155.
[25] J.P. Draayer, Y. Akiyama, Wigner and Racah coefficients for SU_3, J. Math. Phys. 14 (1973) 1904.
[26] Y. Akiyama, J.P. Draayer, A user's guide to FORTRAN programs for Wigner and Racah coefficients of SU(3), Comput. Phys. Commun. 5 (1973) 405.
[27] G. Rosensteel, Analytic formulae for interacting boson model matrix elements in the su(3) basis, Phys. Rev. C 41 (1990) 730.
[28] F. Iachello, N.V. Zamfir, R.F. Casten, Phase coexistence in transitional nuclei and the interacting-boson model, Phys. Rev. Lett. 81 (1998) 1191.
[29] J. Jolie, P. Cejnar, J. Dobeš, Phase coexistence in the interacting boson model and ^{152}Sm, Phys. Rev. C 60 (1999) 061303.
[30] L.R. Dai, F. Pan, L. Liu, L.X. Wang, J.P. Draayer, Alternative characterization of the spherical to axially deformed shape-phase transition in the interacting boson model, Phys. Rev. C 86 (2012) 034316.
[31] K. Yoshida, T. Nakatsukasa, Shape evolution of giant resonances in Nd and Sm isotopes, Phys. Rev. C 88 (2013) 034309.
[32] J. Kvasil, V.O. Nesterenko, A. Repko, W. Kleinig, P.-G. Reinhard, Deformation-induced splitting of the isoscalar E0 giant resonance: Skyrme random-phase-approximation analysis, Phys. Rev. C 94 (2016) 064302.
[33] M. Itoh, H. Sakaguchi, M. Uchida, T. Ishikawa, T. Kawabata, T. Murakami, H. Takeda, T. Taki, S. Terashima, N. Tsukahara, Y. Yasuda, M. Yosoi, U. Garg, M. Hedden, B. Kharraja, M. Koss, B.K. Nayak, S. Zhu, H. Fujimura, M. Fujiwara, K. Hara, H.P. Yoshida, H. Akimune, M.N. Harakeh, M. Volkerts, Systematic study of $L \leq 3$ giant resonances in Sm isotopes via multipole decomposition analysis, Phys. Rev. C 68 (2003) 064602.
[34] National Nuclear Data Center, Brookhaven National Laboratory, Nudat 3.0 (nuclear structure and decay data), https://www.nndc.bnl.gov/nudat3/.
[35] T. Kibédi, R.H. Spear, Electric monopole transitions between 0^+ states for nuclei throughout the periodic table, At. Data Nucl. Data Tables 89 (2005) 77.
[36] P.E. Garrett, Characterization of the β vibration and 0^+_2 states in deformed nuclei, J. Phys. G, Nucl. Part. Phys. 27 (2001) R1–R22.
[37] P.E. Garrett, W.D. Kulp, J.L. Wood, D. Bandyopadhyay, S. Choudry, D. Dashdorj, S.R. Lesher, M.T. McEllistrem, M. Mynk, J.N. Orce, S.W. Yates, New features of shape coexistence in ^{152}Sm, Phys. Rev. Lett. 103 (2009) 062501.